Update on CTTS disruption modeling efforts

Jacob King (Tech-X)

Eric Howell, Scott Kruger
(Tech-X)
Cihan Ackay, Dan Barnes, John Finn
(Tibbar Tech)

CTTS Meeting
Apr. 22nd 2018

Work funded by US DOE FES

Update on efforts in two topical areas

- Generating equilibria for NTM studies
  - Primary: E. Howell
- Accurate boundary element calculations for resistive-wall calculations
  - Primary: D. Barnes

Tearing modes are a leading cause of disruptions in tokamaks.

- Small islands are often born rotating with the plasma.
- NTV and Maxwell torques slow the island rotation.
- Islands may lock if torques are strong enough.
- Disruptions often occur after locking.

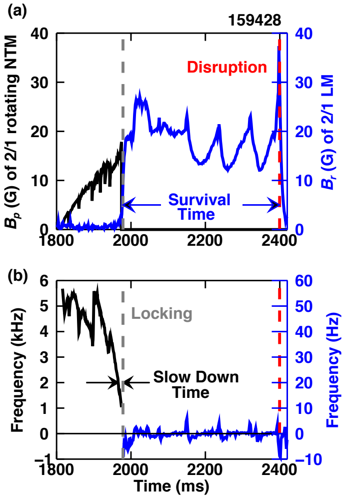

R. Sweeney 2017

Start-up is an example where error-fields are a concern for ITER.

- Error-fields exert a Maxwell torque that slows mode rotation
  - Locking occurs if error fields exceed a critical magnitude
- As designed ITER's error-field correction system will be able to reduce error-fields to
$$\frac{\delta b}{B} \approx 5 \times 10^{-5}$$
- Extrapolation from current experiments predicts a threshold for mode locking during start-up between:
$$1.3 \times 10^{-5} \lesssim \left(\frac{\delta b}{B}\right)_{crit} \lesssim 2.7 \times 10^{-4}$$
- Fitzpatrick's nonlinear analytic theory predicts a locking threshold:[1]
$$\left(\frac{\delta b}{B}\right)_{crit} \approx 5 \times 10^{-5}$$
- Here we plan of using simulations to study the scaling of Maxwell torques and locking thresholds in realistic equilibria

[1] R Fitzpatrick, PPCF 2012

Roadmap for Maxwell torque scaling and locking studies

- Identify equilibria for study
  - Want a tearing mode unstable case: $\Delta' > 0$
  - No pedestal to avoid ELM's
  - Generating model equilibrium is easier than finding a good reconstruction
- Use heuristic neoclassical viscosity to rapidly explore the parameter space.
  - The long term goal is to use continuum kinetic closures
  - Kinetic closures are computationally expensive
- Run initial simulations without flow or error fields
  - Not interested in the formation of the islands, so use tricks to speed up computation
  - Add flows and RMPs after islands saturate

Step 1: Generate tearing unstable equilibria with ITER like shaping.

- Use experimental coil currents from DIII-D with ITER shaping
  - Also interested in using ITER's coil
- Adjust equilibrium F and P profiles to create tearing unstable cases
  - Target a 2/1 or 3/2 mode
  - Use resistive DCON to quickly assess the stability
- Requires incorporating the free boundary solver into fg_nimeq
- Scale unstable equilibrium to JET and ITER length scales.
  - Fix ϵ and β_N
  - Scale R, $F(\psi)$, $P(\psi)$, I_c, etc consistently

Step 2: Revive the heuristic neoclassical viscosity to rapidly explore the parameter space[2].

- The heuristic closure has the form:

$$\nabla \cdot \vec{\vec{\Pi}}_\alpha = n m_\alpha \mu_\alpha \left\langle B^2 \right\rangle \frac{\vec{V}_\alpha \cdot \vec{e}_\Theta}{\left(\vec{B} \cdot \vec{e}_\Theta\right)^2} \vec{e}_\Theta$$

- The dampening frequency, μ_α, can be used to control the island size.
  - Normalize island widths across cases (DIII-D, JET, and ITER)
  - Study small, medium, and large saturated islands
- The heuristic closures mimics the dominant neoclassical effects
  - Only exerts a force in the poloidal direction
  - Poloidal flow dampening
  - Polarization current
  - Bootstrap current

[2] T. A. Gianakon, S. E. Kruger, and C. C. Hegna, POP 2002

NIMUW's free boundary solver has been incorporated into fg_nimeq

- Simultaneously solve for $\Lambda = \frac{\psi}{R^2}$ and $K = \frac{\mu_0 J_\phi}{R}$

$$\nabla \cdot R^2 \nabla \Lambda = -FF' - \mu_0 R^2 P'$$
$$R^2 K = -FF' - \mu_0 R^2 P'$$

- The boundary flux $\Lambda_b = \frac{\psi_b}{R^2}$ is solved simultaneously with the interior flux:

$$\Lambda_b = -\frac{1}{4\pi R_b}\left[\sum_{quad} M_{bq} K_q + \sum_{coils} M_{bc} I_c\right]$$

- The response matrices M are computed at initialization.
- This method eliminates the need for nested iterations that are traditionally used during free boundary solves.

Vertical instability prevents the free boundary solver from converging.

Fixed Boundary RB_ϕ

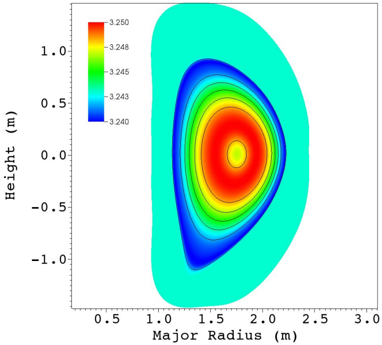

Free Boundary RB_ϕ

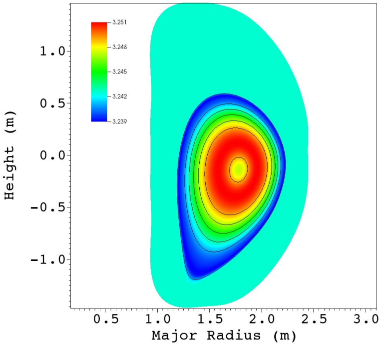

- The free boundary solver is tested using a DIII-D reconstruction
- Free boundary calculations use reconstructed F and P profiles and the experimental PF coil currents
- Free boundary plot shows RB_ϕ after the 10th iteration.
- NIMUW uses up-down symmetry to stabilize vertical motion

A proportional-integral-derivative (PID) controller provides position control.

- Independent vertical and radial feedback systems use a generalization of the algorithm described in Jardin's textbook[3]:

$$\delta I_c^n = \underbrace{\alpha_1 \Delta\psi^n}_{\text{proportional}} + \underbrace{\alpha_2 \left(\Delta\psi^n - \Delta\psi^{n-1}\right)}_{\text{derivative}} + \underbrace{\alpha_3 \sum \Delta\psi^i}_{\text{integral}}$$

$$\Delta\psi \equiv \psi\left(R_1, Z_1\right) - \psi\left(R_2, Z_2\right)$$

- Feedback system is unstable when only the proportional term is used.
- The derivative term provides dampening.
  - Critical for stabilizing the alogrithm
- The integral term has been implemented but needs testing.
- Feedback parameters, α_n, are normalized by the coils response function.

[3] S. Jardin, Computational Methods in Plasma Physics, 2010

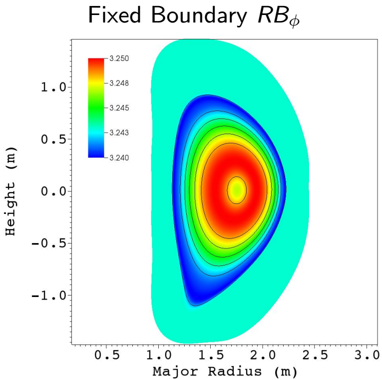

- The free-boundary solver reproduces the original reconstructed equilibrium
- Two vertically aligned equilibrium coils are also used for both radial and vertical position control.
- Feedback current is 3% of the total current in the two feedback coils.

Model equilibria are generated by prescribing F and P profiles

Reconstructed EQ Pressure

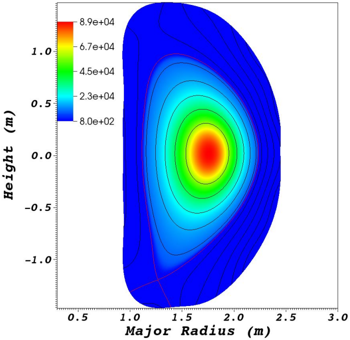

Model EQ Pressure

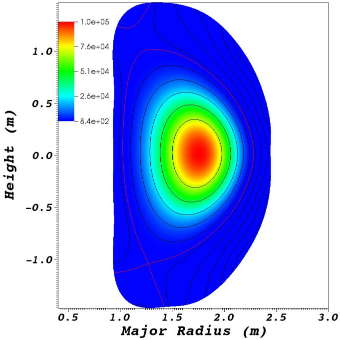

- Model pressure profile: $P = P_0 \left(1 - \hat{\psi}\right)^2 + P_{open}$
- Free-boundary solver also outputs EFIT eqdsk file.
  - Use resistive DCON to assess stability

Conclusions/Future Work

- Beginning Maxwell torque scaling and mode locking studies
  - Locked modes are a concern for ITER
- fg_nimeq has been modified to generate free boundary equilibria
  - PID controller provides position control
  - Shape control may be needed in future
- Plan on using free-boundary solver to generate model equilibria for study
  - Start with experimental coil currents with ITER shaping
  - Modify F and P profiles to generate tearing unstable cases

Prior work coupling NIMROD to a boundary element solution for a resistive wall solution shows poor convergence

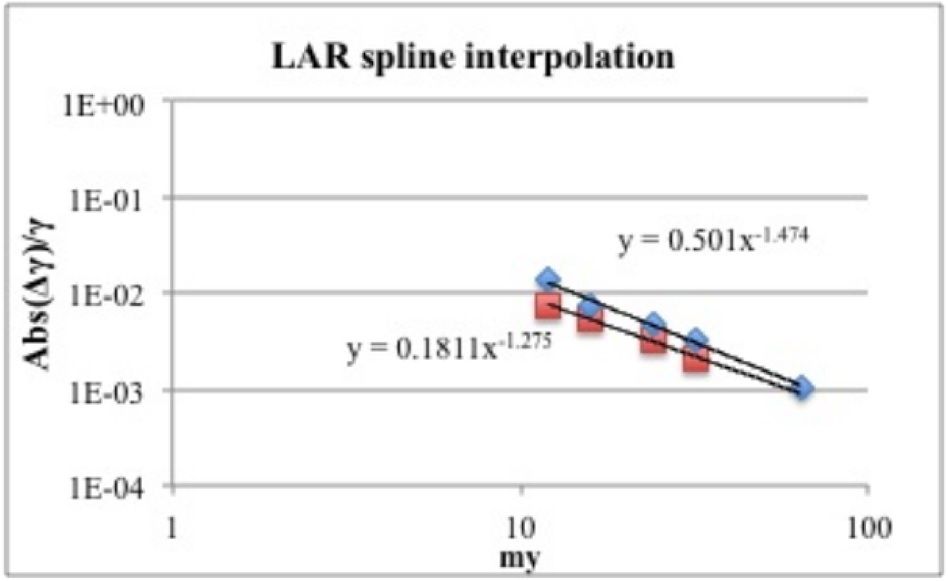

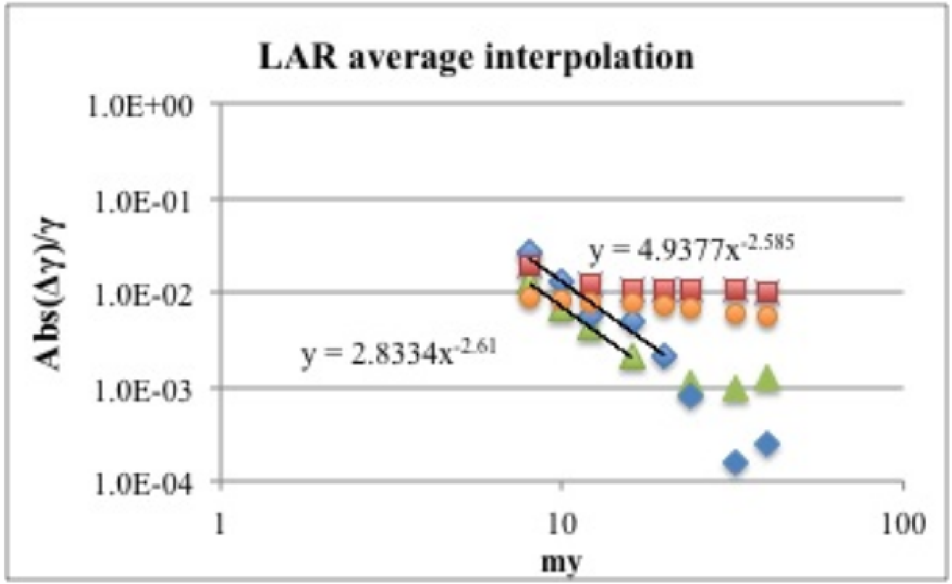

Convergence is only slightly better than 2nd order with high-order elements

Hypothesis: 2nd order methods used in GRIN limit convergence

Challenge: Need more accurate boundary element method for integration with logarithmic singularities

Improve R-wall algorithm

- Desired – *n*th-order convergence (*n* up to 6 or so)

  or

- Round-off-ish accuracy
- Components of boundary integral approach
  - Free-space Green's function
  - Approximate integrals (logarithmic singularity)
  - Matrix inversion and algebra
  - Remainder of algorithm

nimset time

nimrod time

Work to date

- Implemented Young & Martinsson quadrature
- Tested FE direct integration version

$$M_{ii'} = \int d\xi J b_i \int d\xi ' J ' b_i '$$

  – Symmetrized showed jaggies
  – Asymmetric showed 1st order convergence

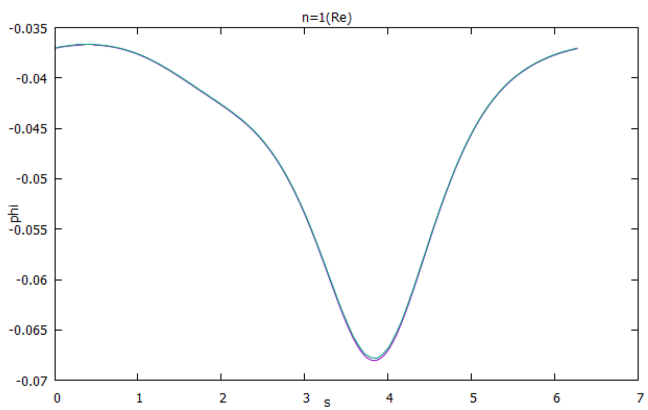

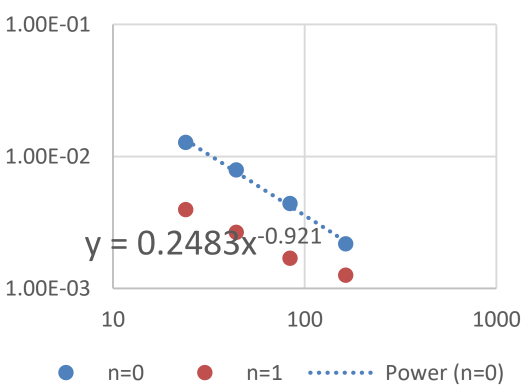

Convergence of boundary solution

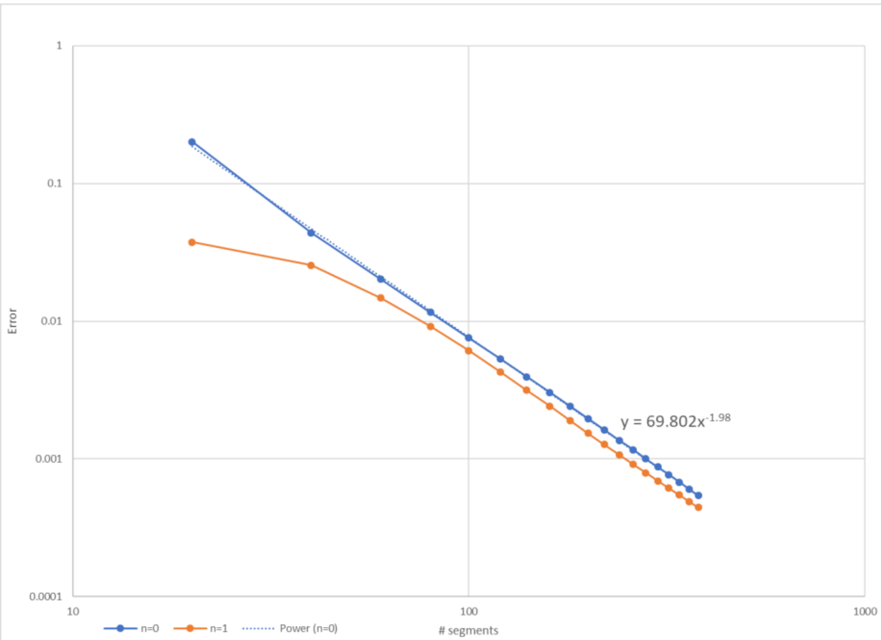

Function

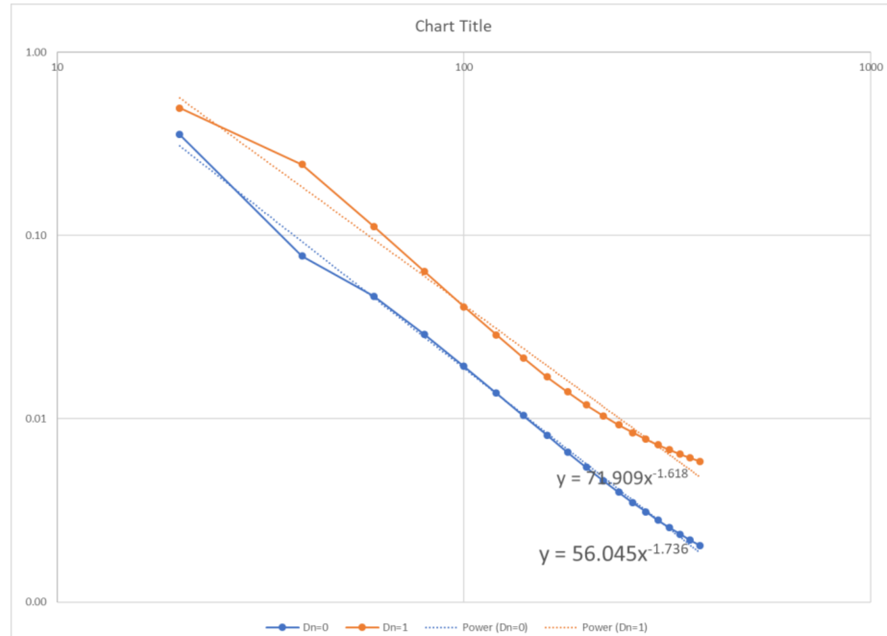

Derivative

Vacuum solver – Green’s functions

MATHEMATICS OF COMPUTATION
Volume 80, Number 275, July 2011, Pages 1725–1743
S 0025-5718(2011)02455-5
Article electronically published on February 1, 2011

PRECISE AND FAST COMPUTATION OF THE GENERAL COMPLETE ELLIPTIC INTEGRAL OF THE SECOND KIND

TOSHIO FUKUSHIMA

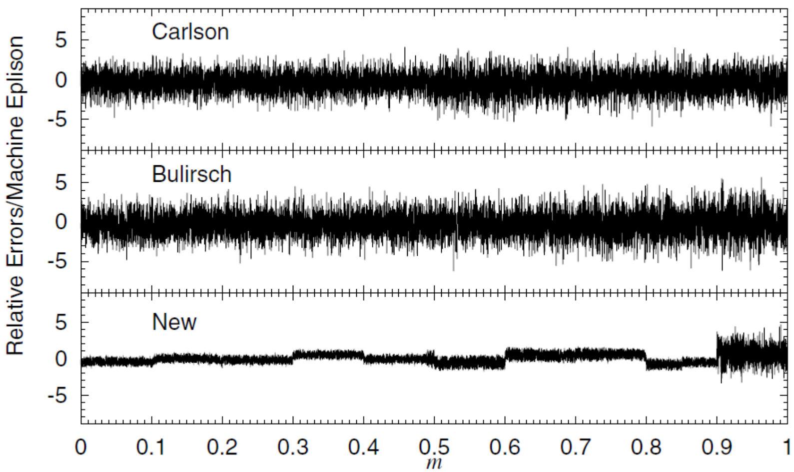

TABLE 7. Coefficients of Taylor Expansion Polynomials of $B(m)$ and $D(m)$: $0.4 < m \leq 0.5$

j	B_j	D_j
0	0.839479570270612971	0.974404366546369673
1	0.149916440306396336	0.613246805394160910
2	0.090831935819428835	0.671096669502166996
3	0.080347033483341786	0.870727620185086140
4	0.085638440500470454	1.229542231202690761
5	0.101954725932990372	1.826605967544420569
6	0.130574811533616015	2.806934530997762740
7	0.176105076358849928	4.418789329084028134
8	0.246835164402955447	7.083236057478765325
9	0.356424476867718855	11.515088120557558294
10	0.527002562230102743	18.931511185999927464
11	0.794389634259304750	31.411996938204963888
12	1.216762532429718021	52.520729454575828854
13		88.384854735065298806
14		149.566374493980478784
15		254.317908431041171743

Vacuum solver – Green's functions

- $n = 0$ & $n = 1$ use elliptic integrals
- $n > 1$ by recursion

$$s(\boldsymbol{x}, \boldsymbol{x}') = \frac{1}{4\pi|\boldsymbol{x} - \boldsymbol{x}'|} = \frac{1}{4\pi^2\sqrt{rr'}} \sum_{n\in\mathbb{Z}} e^{in(\theta-\theta')} \mathcal{Q}_{n-1/2}(\chi)$$

$$\frac{\partial\chi}{\partial r'} = \frac{(r')^2 - r^2 - (z - z')^2}{2r(r')^2},$$

$$\frac{\partial\chi}{\partial z'} = \frac{z' - z}{rr'},$$

$$\mathcal{Q}_{-1/2}(\chi) = \mu K(\mu),$$

$$\mathcal{Q}_{1/2}(\chi) = \chi\mu K(\mu) - \sqrt{2(\chi + 1)}E(\mu),$$

$$\mathcal{Q}_{-n-1/2}(\chi) = \mathcal{Q}_{n-1/2}(\chi),$$

$$\mathcal{Q}_{n-1/2}(\chi) = 4\frac{n-1}{2n-1}\chi\mathcal{Q}_{n-3/2}(\chi) - \frac{2n-3}{2n-1}\mathcal{Q}_{n-5/2}(\chi),$$

$$\frac{\partial\mathcal{Q}_{n-1/2}(\chi)}{\partial\chi} = \frac{2n-1}{2(\chi^2-1)}\left(\chi\mathcal{Q}_{n-1/2} - \mathcal{Q}_{n-3/2}\right),$$

Vacuum solver – Integrals

A DIRECT SOLVER FOR THE RAPID SOLUTION OF BOUNDARY INTEGRAL EQUATIONS ON AXISYMMETRIC SURFACES IN THREE DIMENSIONS

Patrick Young and Per-Gunnar Martinsson
Dept. of Applied Mathematics, Univ. of Colorado at Boulder, Boulder, CO 80309-0526

Abstract: A scheme for rapidly and accurately computing solutions to boundary integral equations (BIEs) on rotationally symmetric surfaces in $\mathbb{R}^3$ is presented. The scheme uses the Fourier transform to reduce the original BIE defined on a surface to a sequence of BIEs defined on a generating curve for the surface. It can handle loads that are not necessarily rotationally symmetric. Nyström discretization is used to discretize the BIEs on the generating curve. The quadrature used is a high-order Gaussian rule that is modified near the diagonal to retain high-order accuracy for singular kernels. The reduction in dimensionality, along with the use of high-order accurate quadratures, leads to small linear systems that can be inverted directly via, *e.g.*, Gaussian elimination. This makes the scheme particularly fast in environments involving multiple right hand sides. It is demonstrated that for BIEs associated with Laplace's equation, the kernel in the reduced equations can be evaluated very rapidly by exploiting recursion relations for Legendre functions. Numerical examples illustrate the performance of the scheme; in particular, it is demonstrated that for a BIE associated with Laplace's equation on a surface discretized using 320 000 points, the set-up phase of the algorithm takes 2 minutes on a standard desktop, and then solves can be executed in 0.5 seconds.

N_{P}	$2N_{\mathrm{F}}+1$				
-	25	50	100	200	400
5	1.93869e-04	4.10935e-07	5.37883e-08	5.37880e-08	5.37880e-08
10	1.93869e-04	4.10513e-07	3.27169e-12	6.72270e-13	6.72270e-13
20	1.93869e-04	4.10513e-07	3.30601e-12	1.66132e-13	1.66132e-13
40	1.93869e-04	4.10513e-07	3.23162e-12	8.28568e-14	8.28568e-14
80	1.93869e-04	4.10512e-07	2.92918e-12	2.92091e-13	2.92091e-13

TABLE 3. Error in internal Dirichlet problem solved on domain (a) in Figure 6.1.

APPENDIX OF QUADRATURE NODES AND WEIGHTS

10 Point Gauss-Legendre Rule for integrals of the form $\int_{-1}^{1} f(x)\,dx$	
NODES	WEIGHTS
-9.739065285171716e-01	6.667134430868814e-02
-8.650633666889845e-01	1.494513491505806e-01
-6.794095682990244e-01	2.190863625159820e-01
-4.333953941292472e-01	2.692667193099963e-01
-1.488743389816312e-01	2.955242247147529e-01
1.488743389816312e-01	2.955242247147529e-01
4.333953941292472e-01	2.692667193099963e-01
6.794095682990244e-01	2.190863625159820e-01
8.650633666889845e-01	1.494513491505806e-01
9.739065285171716e-01	6.667134430868814e-02

20 point quadrature rule for integrals of the form $\int_{-1}^{1} f(x) + g(x)\log\lvert x_1 - x\rvert\,dx$, where x_1 is a Gauss-Legendre node	
NODES	WEIGHTS
-9.981629455677877e-01	4.550772157144354e-03
-9.915520723139890e-01	8.062764683328619e-03
-9.832812993252168e-01	7.845621096866406e-03
-9.767801773920733e-01	4.375212351185101e-03
-9.717169387169078e-01	1.021414662954223e-02
-9.510630103726074e-01	3.157199356768625e-02
-9.075765988474132e-01	5.592493151946541e-02
-8.382582352569804e-01	8.310260847601852e-02
-7.408522006801963e-01	1.118164522164500e-01
-6.147619568252419e-01	1.401105427713687e-01
-4.615244999958006e-01	1.657233639623953e-01
-2.849772954295424e-01	1.863566566231937e-01
-9.117593460489747e-02	1.999093145144455e-01
1.119089520342051e-01	2.046841584582030e-01
3.148842536644393e-01	1.995580161940930e-01
5.075733846631832e-01	1.841025430283230e-01
6.797470718157004e-01	1.586456191174843e-01
8.218833662202629e-01	1.242680229936124e-01
9.258924858821892e-01	8.273794370795576e-02
9.857595961761246e-01	3.643931593123844e-02

Vacuum solver – Integrals

- Testing in stand-alone code
  - $n = 0$ & $n = 1$ so far
  - Manufacture solution using several random sources inside torus
  - Give $\partial_n \phi$ solve for ϕ compare
- Issues
  - Young & Martinsson use Nystrom method (collocation)
  - We need (eventually) FE method
  - Interpolation between various meshes

Manufactured solution

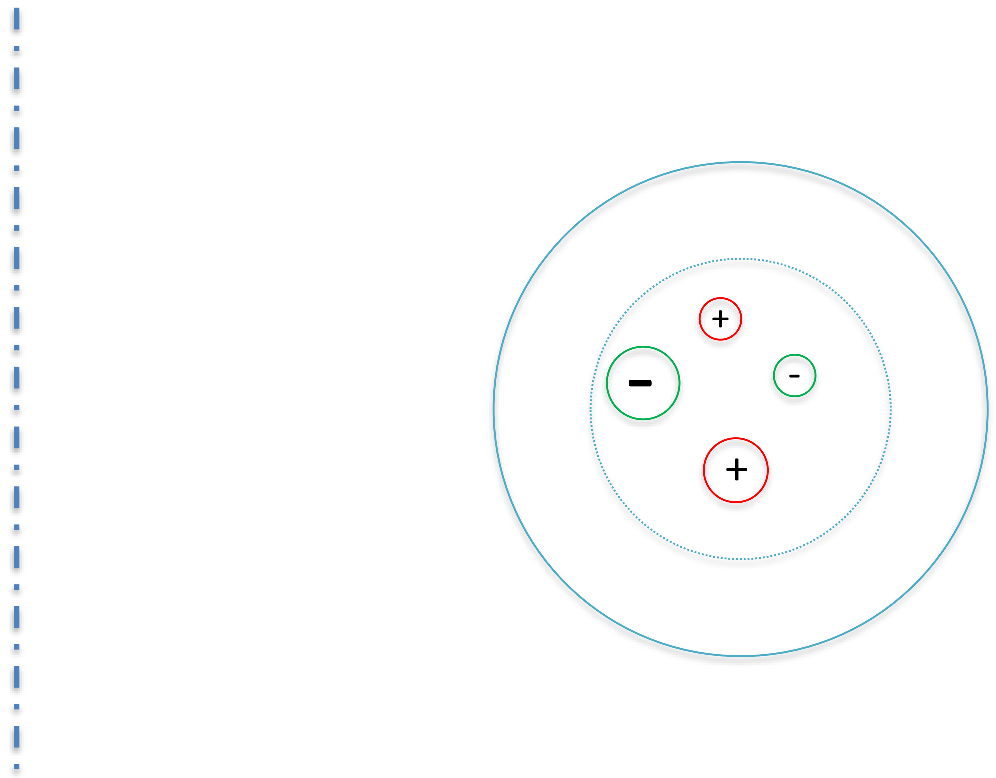

Vacuum solver – Integrals

- Status
  - Progress
  - Problems (bugs)
  - Higher-order not yet

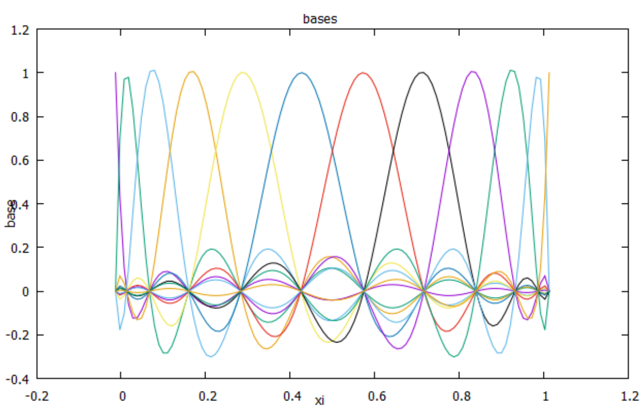

Lagrange interpolation on G-L nodes

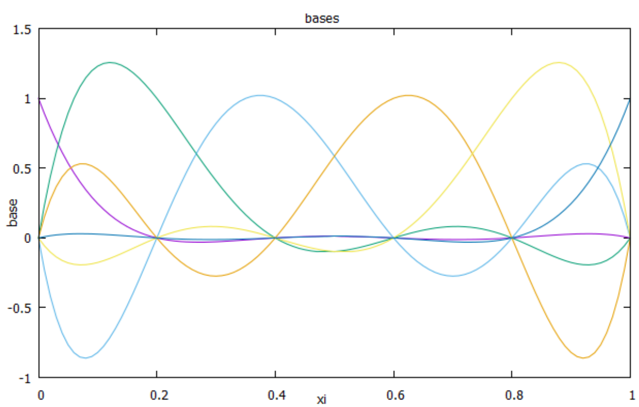

Lagrange interpolation on deg 5 regular

Present

- Testing Nystrom method on G-L mesh
  - Found description of interpolation vague
  - So – used different method near ends of each segment
  - Still buggy code, so need week or two more work
- Reproduce Y & M high-accuracy results
- Interpolate 2 ways to FE?
- Understand issues with direct FE formulation

Summary

- Progress on-going on infrastructure to enable disruption simulations
- Generation of tearing mode unstable cases
- Accurate resistive-wall response matrix